

Schottky-barrier height modulation of metal/ $\text{In}_{0.53}\text{Ga}_{0.47}\text{As}$ interfaces by insertion of atomic-layer deposited ultrathin Al_2O_3

Runsheng Wang^{a)}

School of Electrical and Computer Engineering and Birck Nanotechnology Center, Purdue University, West Lafayette, Indiana 47906 and Institute of Microelectronics, Peking University, Beijing 100871, China

Min Xu and Peide D. Ye

School of Electrical and Computer Engineering and Birck Nanotechnology Center, Purdue University, West Lafayette, Indiana 47906

Ru Huang

Institute of Microelectronics, Peking University, Beijing 100871, China

(Received 21 July 2010; accepted 24 June 2011; published 2 August 2011)

The improvement of the metal/ InGaAs interface is essential for the future application of InGaAs metal source/drain Schottky-barrier metal-oxide-semiconductor field-effect-transistors. In this article, on $\text{In}_{0.53}\text{Ga}_{0.47}\text{As}$, the authors examine the recently proposed method of inserting an ultrathin insulator to modulate the effective Schottky-barrier height (SBH) at the metal/semiconductor interface. Both n-type and p-type $\text{In}_{0.53}\text{Ga}_{0.47}\text{As}$ are investigated by inserting an atomic-layer deposited Al_2O_3 interlayer. The results indicate that SBH modulation is more effective at the n- InGaAs interface than the p- InGaAs interface for the same Al_2O_3 thickness. However, the Fermi level at the metal/ InGaAs interface is still weakly pinned even after inserting 2 nm Al_2O_3 . The mechanism of the SBH modulation could be attributed to the creation of an electric dipole at the $\text{Al}_2\text{O}_3/\text{InGaAs}$ interface, which induces a barrier shift. © 2011 American Vacuum Society. [DOI: 10.1116/1.3610972]

I. INTRODUCTION

The desire for enhanced carrier transport properties in high-performance complementary metal-oxide-semiconductor (CMOS) devices has led to increased interest in non-Si channel materials such as Ge and III-V compound semiconductors. Recently, great attention has been given to In-rich InGaAs as an alternative n-channel material due to its high electron mobility, high saturation velocity, and appropriate bandgap for high-speed and low-power applications.¹⁻⁴ Much progress has been made in growing high-quality high-k gate dielectrics on InGaAs using atomic-layer deposition (ALD) in order to solve the Fermi level pinning issue in metal/oxide/III-V systems.^{1,3,4} Historically this issue was the main technological bottleneck for demonstrating III-V metal-oxide-semiconductor field-effect transistors (MOSFETs). However, another bottleneck is poor dopant activation in III-V semiconductors which often results in relatively high source/drain (S/D) series resistances in devices. The metal S/D Schottky-barrier MOSFET (SB-FET),⁵ which is schematically shown in Fig. 1(a), has been proposed as a potential solution.⁶ Besides reduced S/D resistances and a naturally abrupt junction profile, the low thermal budget of SB-FETs also makes it attractive for integration with a high-k/metal-gate. Implementing a SB-FET using a III-V semiconductor can be difficult because the Fermi levels at metal/III-V interfaces are generally pinned. Therefore, the

Schottky-barrier height (SBH) modulation technique is needed when implementing the SB-FET for most III-V materials.

Two methods have been proposed to modulate the effective SBH at the metal/semiconductor interface. One method is the introduction of appropriate dopants at the semiconductor surface. This approach, known as dopant segregation, has been successfully implemented for Si.⁷ Another approach is to insert an ultrathin insulator between the metal and the semiconductor. This approach has been demonstrated with Si,⁸ Ge,^{9,10} and GaAs.^{11,12} Considering the relatively low solid solubility of impurities in InGaAs and the processing complexity of the first approach, the second approach is more suitable for InGaAs . In Ref. 8, the mechanism of the SBH modulation is proposed to be the releasing of the initial Fermi level pinning at the metal/Si interface. If this approach also works for InGaAs , as illustrated in Figs. 1(b) and 1(c), the thin insulator can reduce the Fermi level pinning caused by metal-induced gap states (MIGS)^{13,14} by suppressing the metal wave function penetration into the semiconductor band gap and also by passivating the interface states. Therefore, in this article, we examine the effectiveness of this method on both n-type and p-type InGaAs by inserting an ultrathin Al_2O_3 interlayer. The Al_2O_3 interlayer is deposited by the ALD approach, which is particularly suitable to form the ultrathin oxide layers needed for this method.

II. EXPERIMENT

Both n-type and p-type $\text{In}_{0.53}\text{Ga}_{0.47}\text{As}$ (100) epilayers with a doping concentration of $\sim 10^{17}/\text{cm}^3$ were grown on InP

^{a)}Electronic mail: wrs@pku.edu.cn

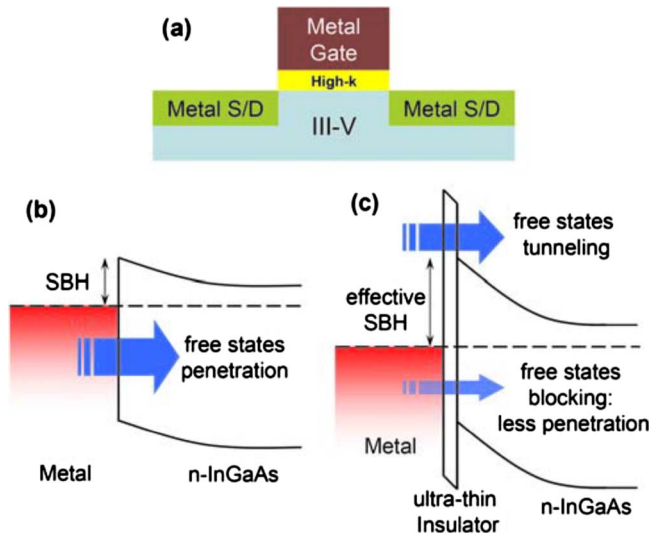


FIG. 1. (Color online) (a) Schematic view of a high- k /III-V SB-FET. The principle of the effective SBH modulation if following the MIGS theory as follows: (b) In direct metal/semiconductor contact, metal wave function decays into the semiconductor and creates MIGS that results in Fermi level pinning at the interface. (c) Inserting an ultrathin insulator can reduce MIGS and thus modulate the effective SBH.

substrates by molecular beam epitaxy. The InGaAs epilayers were first degreased in acetone and methanol. The surface pretreatment was done by dipping the samples in a $\text{HCl}:\text{H}_2\text{O}=1:1$ solution for 30 s to remove the native oxide, rinsing in flowing DI water, soaking the samples in 29% $(\text{NH}_4)_2\text{S}$ for 10 min at room temperature, and drying. The samples were then loaded into an ASM F-120 ALD system immediately. A 2 nm Al_2O_3 layer was deposited at 300 °C by using trimethylaluminum (TMA) and water (H_2O) precursors. No postdeposition-annealing was performed. Ni, Ti, $\text{Ni}_{0.80}\text{Fe}_{0.20}$, Co, or Cr metal contact and Au capping layer were then deposited by electron-beam evaporation via a shadow mask. Samples without the ultrathin Al_2O_3 interlayer were also fabricated at the same time for comparison. The effective SBH is extracted by the temperature dependent J - V technique.¹⁵

III. RESULTS AND DISCUSSION

Figures 2(a) and 2(b) show the typical J - V characteristics of the fabricated n- and p-type InGaAs Schottky diodes with and without the ultrathin Al_2O_3 layer. Regardless of the difference in metal work function, Ohmic behaviors are observed on all metal/n-InGaAs junctions and rectifying behaviors are obtained on metal/p-InGaAs junctions. Strong Fermi level pinning is observed near the conduction band of $\text{In}_{0.53}\text{Ga}_{0.47}\text{As}$. As shown in Fig. 2(a), after inserting an ultrathin Al_2O_3 layer, the metal/n-InGaAs junction exhibits Schottky performance, indicating the modulation of the effective SBH at the InGaAs interface. The current density of the pure Schottky diode is $J=A^*T^2 \exp(-q\Phi_B/kT) \times [\exp(qV/nkT)-1]$,¹⁶ where A^* is the Richardson constant, T is the temperature, q is the electron charge, Φ_B is the effective SBH, k is the Boltzmann constant, n is the ideality

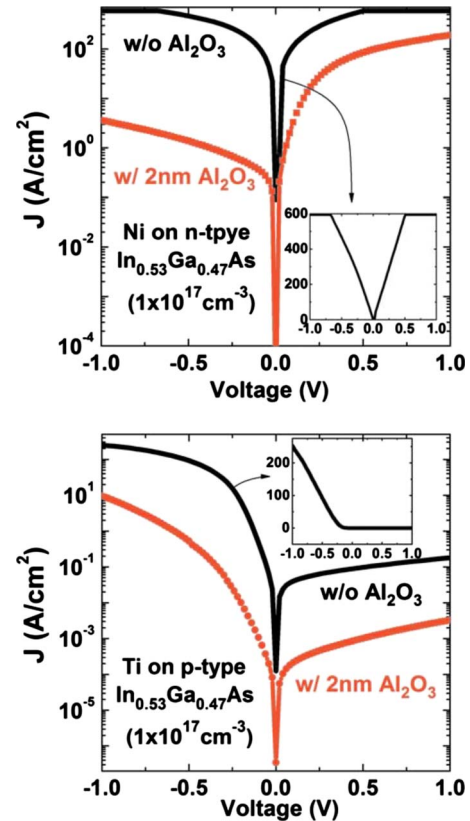


FIG. 2. (Color online) Typical J - V characteristics of (a) n-type and (b) p-type metal/ $\text{In}_{0.53}\text{Ga}_{0.47}\text{As}$ junctions, with and without inserting an ultrathin Al_2O_3 layer between metal and InGaAs interface.

factor, and V is the applied forward voltage. When considering a Schottky diode with an ultrathin insulator, the current can be written as $J'=J \cdot P$,¹⁶ with the tunneling probability $P=\exp(-\sqrt{\zeta}\delta)$, where ζ and δ are the effective barrier and thickness of the inserted interfacial oxide layer. Therefore, for both types of Schottky diodes biased at $V>3kT/q$, the effective SBH can be accurately extracted from the temperature dependence of $\ln(J/T^2)$.

Figures 3(a) and 3(b) plot the extracted effective SBHs as a function of metal work functions on n- and p-type $\text{In}_{0.53}\text{Ga}_{0.47}\text{As}$, respectively, which show different behaviors. For n-InGaAs, a 2 nm Al_2O_3 insertion can increase the effective SBH from near 0 eV (Ohmic) to maximum 0.34 eV. For p-InGaAs, the modulation of SBH is much less effective, which is only 0.05 eV at its maximum. Note that the effective SBH of Ti/InGaAs is distinct from all other metals and is far from satisfying the ideal Schottky–Mott relation. Ti may have this unexpected behavior because its work function (4.33 eV) is outside of the bandgap of $\text{In}_{0.53}\text{Ga}_{0.47}\text{As}$ (which has an electron affinity (χ) of 4.5 eV), while the work functions of the other metals are within the bandgap of $\text{In}_{0.53}\text{Ga}_{0.47}\text{As}$. Also, Ti is a very reactive metal which may reduce the quality of Ti/ Al_2O_3 interface and impact its effective work function.

The observation of the SBH shift by inserting an ultrathin insulator is not fully understood. In a metal/Si system, this effect was attributed to releasing the Fermi level pinning

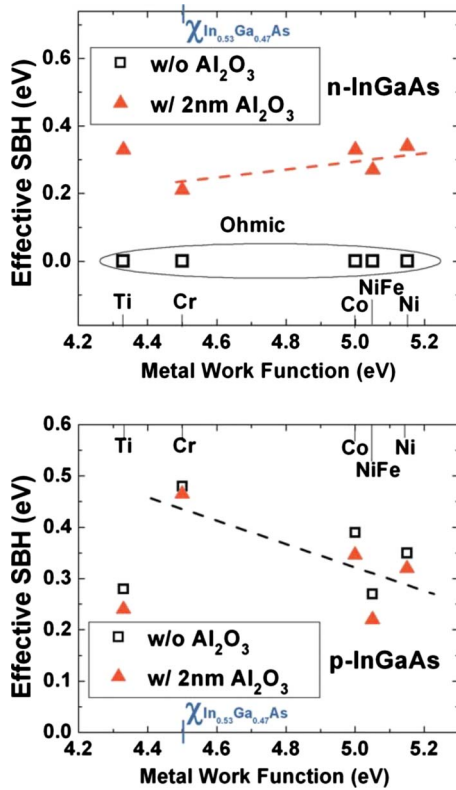


FIG. 3. (Color online) Extracted effective SBH as a function of metal work function on (a) n-type and (b) p-type $\text{In}_{0.53}\text{Ga}_{0.47}\text{As}$. The 2 nm Al_2O_3 passivation increases the effective SBH on n-InGaAs from near 0 eV (Ohmic) to 0.21–0.34 eV, while decreasing the effective SBH on p-InGaAs for less than 0.05 eV.

caused by MIGS.⁸ However, this explanation does not apply to either n- or p-InGaAs with a 2 nm Al_2O_3 interlayer since their SBHs are found to only weakly depend on the metal work function. As shown in Fig. 3, the change of the effective SBH with metal work function is less than 0.3 eV while the metal work function changes by about 0.9 eV. This result implies that there is a large downwards shift of the Fermi level pinning level. The Fermi level could still be weakly pinned after inserting a thin Al_2O_3 , but the Fermi level “pinning position” is altered from near the conduction band to near the midgap. It is interesting to note that similar results can also be found in the published experimental data for metal/Ge system [e.g., see Fig. 2(b) in Ref. 10 and Fig. 14 in Ref. 9], although they show an upward shift of the Fermi level pinning level. Note that the opposite shift direction in Ge is because its initial Fermi level pinning position is near its valance band. This is in great contrast to InGaAs which has an initial Fermi level pinning position near its conduction band.

Therefore, considering that the MIGS model neglects the chemical bond change at the interface, the observed SBH shift in metal/InGaAs could be attributed to the creation of an electric dipole formed at the $\text{Al}_2\text{O}_3/\text{InGaAs}$ interface which changes the atomic structure connected to InGaAs. The inserted Al_2O_3 creates a polar $\text{Al}_2\text{O}_3/\text{InGaAs}$ interface, thus inducing a dipole which leads to a barrier shift, as illus-

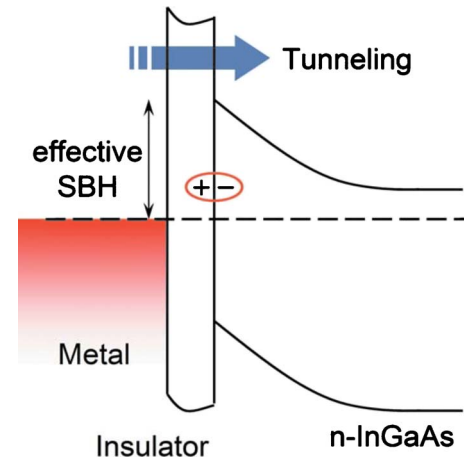


FIG. 4. (Color online) Illustration of the dipole effect at the oxide/InGaAs interface. The inserted Al_2O_3 can create an electric dipole which induces a barrier shift.

trated in Fig. 4. To be more specific, the observed SBH shifts caused by the Al_2O_3 interlayer ($\sim 0.2\text{--}0.3$ eV for n-InGaAs, ~ 0.04 eV for p-InGaAs) is nearly independent of metal choice. This implies that dipoles are formed because the dipole magnitude is independent of metals but strongly dependent on the oxide/semiconductor interface. Thus, the experiments suggest that, for n-InGaAs, the 2 nm Al_2O_3 interlayer introduces a dipole of about $0.2\text{--}0.3$ eV, while for p-InGaAs, it is only about 0.04 eV.

This attribution of the SBH shift on InGaAs to the interface dipole is consistent with bond-polarization theory,¹⁷ and similar to the recent discussions of metal/high-k/ SiO_2/Si systems.¹⁸ The physical origin of the dipole is not well understood. It is related to the minimization of the interface energy and might relate to the redistribution of oxygen across the interface.¹⁹ Further systematic study is needed to more deeply understand the mechanism of dipole formation, for example, by varying oxide type and thicknesses in order to create different interface dipoles with different magnitudes.

In addition, the Fermi level pinning behaviors at the metal/InGaAs interfaces are quite different for n-type and p-type InGaAs. As observed in Fig. 3, even without Al_2O_3 insertion, the SBH of the p-type InGaAs diodes depends on the metal work function more strongly than the n-type InGaAs diodes. This implies that the Fermi level pinning at the interface of metal on p-type InGaAs is not as strong as on n-type InGaAs. We ascribe this to the effect of $(\text{NH}_4)_2\text{S}$ -based pretreatment of the p-type InGaAs surface which is similar to the method for unpinning the Fermi level of p-type InGaAs MOS capacitors.²⁰ Furthermore, even after inserting a 2 nm Al_2O_3 interlayer, the Fermi level is still weakly pinned at the metal/n-InGaAs interfaces for various metals, as shown in Fig. 3(a). This is probably due to the large amount of donor-type interface states after inserting the ultrathin Al_2O_3 without annealing²⁰ or to the redistribution of interface states. On the strongly pinned n-InGaAs surface, the ultrathin insulator cannot fully unpin the metal/n-InGaAs

interface. This difference between n- and p-type InGaAs may be related to the initial position of Fermi levels in the semiconductor bulk. If the semiconductor bulk Fermi level is close to the charge neutrality level (E_{CNL}),^{14,17} then the Fermi level at the interface would be strongly pinned around E_{CNL} . Since the E_{CNL} of InGaAs is near its conduction band, the Fermi level pinning effect in n-type InGaAs could be stronger than p-type InGaAs. In p-type InGaAs, where the Fermi level is initially far away from E_{CNL} , the Fermi level at the interface could be located below E_{CNL} with a certain energy separation and thus less pinned [in particular, with $(\text{NH}_4)_2\text{S}$ passivation], as shown in Fig. 3(b). More work is needed to optimize the process and improve the SBH modulation efficiency.

IV. SUMMARY AND CONCLUSIONS

In summary, a method to change the Fermi level pinning position and SBH modulation effectiveness at metal/InGaAs interfaces is examined by inserting an ultrathin ALD Al_2O_3 interlayer. The results indicate that the SBH modulation is more effective on n-InGaAs interfaces than on p-InGaAs interfaces when using the same Al_2O_3 thickness. However, adding the 2 nm Al_2O_3 interlayer does not fully unpin the Fermi level at the metal/InGaAs interface. The mechanism of the SBH modulation could be attributed to the creation of an electric dipole at the $\text{Al}_2\text{O}_3/\text{InGaAs}$ interface which induces a barrier shift. More work is needed to optimize oxide material and thickness in order to improve the SBH modulation efficiency and/or unpin the Fermi level at the metal/ $\text{In}_{0.53}\text{Ga}_{0.47}\text{As}$ interface while still having a low contact resistance for InGaAs SB-FETs.

ACKNOWLEDGMENTS

This work was supported in part by NSF and the SRC FCRP MSD Focus Center. The authors would like to thank N. J. Conrad for critical reading of the manuscript and the helpful discussions. R. Wang would also like to thank China Scholarship Council.

- ¹Y. Xuan, Y. Q. Wu, and P. D. Ye, *IEEE Electron Device Lett.* **29**, 294 (2008).
- ²T. D. Lin, H. C. Chiu, P. Chang, L. T. Tung, C. P. Chen, M. Hong, J. Kwo, W. Tsai, and Y. C. Wang, *Appl. Phys. Lett.* **93**, 033516 (2008).
- ³N. Goel *et al.*, *Tech. Dig. - Int. Electron Devices Meet.* **2008**, 363.
- ⁴Y. Sun, E. W. Kiewra, J. P. de Souza, J. J. Bucchnano, K. E. Fogel, D. K. Sadana and G. G. Shahidi, *Tech. Dig. - Int. Electron Devices Meet.* **2008**, 367.
- ⁵S. Xiong, T.-J. King, and J. Bokor, *IEEE Trans. Electron Devices* **52**, 1859 (2005).
- ⁶M. Yokoyama *et al.*, *VLSI Symp.* **2009**, 242.
- ⁷M. Awano, H. Onoda, K. Miyashita, K. Adachi, Y. Kawase, K. Miyano, H. Yoshimura, and T. Nakayama, *VLSI Symp.* **2008**, 24.
- ⁸D. Connelly, C. Faulkner, D. E. Grupp, and J. Harris, *IEEE Trans. Nanotechnol.* **3**, 98 (2004).
- ⁹M. Kobayashi, A. Kinoshita, K. Saraswat, H.-S. P. Wong, and Y. Nishi, *VLSI Symp.* **2008**, 54.
- ¹⁰T. Nishimura, K. Kita, and A. Toriumi, *App. Phys. Express* **1**, 051406 (2008).
- ¹¹J. Hu, X. Guan, D. Choi, J.S. Harris, K. Saraswat, and H.-S. P. Wong, *VLSI-TSA* **2009**, 123.
- ¹²J. Hu, K. C. Saraswat, and H.-S. P. Wong, *J. Appl. Phys.* **107**, 063712 (2010).
- ¹³V. Heine, *Phys. Rev. A* **138**, A1689 (1965).
- ¹⁴J. Tersoff, *Phys. Rev. Lett.* **52**, 465 (1984).
- ¹⁵D. K. Schroder, *Semiconductor Material and Device Characterization*, 3rd ed. (Wiley, New York, 2006), pp. 157–164.
- ¹⁶S. M. Sze and K. K. Ng, *Physics of Semiconductor Devices Characterization*, 3rd ed. (Wiley, New York, 2007), pp. 160–170.
- ¹⁷R. T. Tung, *Mater. Sci. Eng., R.* **35**, 1 (2001).
- ¹⁸B. E. Coss *et al.*, *VLSI Tech. Dig.* **2009**, 104.
- ¹⁹K. Kita, and A. Toriumi, *Tech. Dig. - Int. Electron Devices Meet.* **2008**, 29.
- ²⁰Y. Xuan, Y. Q. Wu, T. Shen, T. Yang, and P. D. Ye, *Tech. Dig. - Int. Electron Devices Meet.* **2007**, 637.